Int. J. Electrochem. Sci., 8 **(2013)** 4654 - 4669

International Journal of
ELECTROCHEMICAL
SCIENCE
www.electrochemsci.org

A New Hybrid Polyhedral Cubic Silsesquioxane Chemically Modified with 4-amino-5-(4-pyridyl)-4*H*-1,2,4-triazole-3-thiol (APTT) and Copper Hexacyanoferrate(III) for Voltammetric Determination of Nitrite

Layciane Aparecida Soares, Tayla Fernanda Serantoni da Silveira, Daniela Rodrigues Silvestrini, Urquisa de Oliveira Bicalho, Newton Luiz Dias Filho, Devaney Ribeiro do Carmo[*]

Faculdade de Engenharia de Ilha Solteira UNESP - Univ Estadual Paulista, Departamento de Física e Química, Av. Brasil Centro, 56 CEP 15385-000, Ilha Solteira, SP, Brazil. Fax: +55 (18) 3742-4868.
[*]E-mail: docarmo@dfq.feis.unesp.br

Received: 27 January 2013 / *Accepted:* 5 March 2013 / *Published:* 1 April 2013

This paper describes the preparation, and voltammetric application of a hybrid nanocomposite formed by interaction of a octa(3-chloropropyl)octasilsesquioxane (SS) modified with 4-amino-5-4 (pyridyl)-4*H*-1,2,4-triazole-3-thiol (SA), and its subsequent reactions in two steps, first with copper and so hexacyanoferrate (III) (CuHSA). The precursors and CuHSA were initially characterized by by Fourier transform infrared spectra (FTIR). This composite was incorporated into a graphite paste electrode and the electrochemical behavior studies were conducted with cyclic voltammetry. The cyclic voltammogram of the modified graphite paste electrode with CuHSA, showed one redox couple with formal potential $E^{\theta'}$= 0.75V *vs* $Ag/AgCl_{(sat)}$ (KCl 1.0 mol L^{-1}; v = 20 mV s^{-1}) attributed to the redox process $Fe^{(II)}(CN)_6$ / $Fe^{(III)}(CN)_6$ of the binuclear complex formed. The redox couple presents an electrocatalytic response for determination of nitrite. The modified graphite paste electrode showed a linear response of 1.0×10^{-5} to 5.0×10^{-3} mol L^{-1}. The method has a detection limit of 3.57×10^{-4} mol L^{-1}, standard deviation of 1.5% for n=3 with an amperometric sensitivity 30.00 mA/mol L^{-1} to nitrite. The modified electrode was electrochemically stable and showed good reproducibility.

Keywords: Octa(3-chloropropyl)octasilsesquioxane;4-amino-5-4(pyridyl)-4*H*-1,2,4-triazole-3-thiol;voltammetry; electrocatalysis; nitrite

1. INTRODUCTION

Due to general interest in the hybrid materials a great variety of hybrid building blocks are nowadays available. The hybrid materials properties are different from those displayed by their precursors, and new properties (e.g., electrical, magnetic) are acquired resulting from the synergy

between organic and inorganic components. In this context a wide variety of building blocks of inorganic and organic hybrids are now available [1]. Among the hybrid materials, the new class of inorganic-organic silica based, called of silsesquioxanes offer many applications in different field, that is extremamely described in recent reviews [2, 3].

Silsesquioxanes are nanostructured compounds, of the three-dimensional oligomeric organosiliceous compounds with the which have the empirical formula $(RSiO_{1.5})_n$, where R can be a hydrogen or any organic group such as alkyl, methyl, aryl, vinyl, phenyl, arylene or any organofunctional derivative thereof [2-6] and *n* is an integer number that can vary ($n \geq 4$), but it is usually 6, 8 or 10 [3]. Very important properties are attributed to reactions through of pendant groups (organic substituents). These peripheral groups can be totally hydrocarbon in nature or they can embody a range of polar structures and functional groups.

The advantages of using silsesquioxane rather than other molecules, such as clays, carbon fibers and carbon nanotubes, is because they are much smaller and have a monodispersed size, low density, and are readily modified chemically to generate a series of reactive compounds with specific substituents to suit a particular application [3]. When functionalized, silsesquioxanes can improve their mechanical and thermal properties [2, 5, 6] and their oxidative resistance [2]. The silsesquioxanes with "cage" structures are also known as polyhedral oligomeric silsesquioxanes (POSS), and are widely studied because of their well-defined and highly symmetric structure.The derivatives of POSS can have a hybrid architecture (inorganic/organic) with an internal inorganic structure formed by silicon and oxygen, which is externally covered by organic substituents [7], allowing to obtain multifunctional materials with intermediate properties between those of organic polymers and of ceramics. These materials are prepared by functionalization reactions in which the organic compound is bonded to the peripheral groups of POSS. Additionally different from traditional organic compounds, the derivatives of POSS have the advantage of, besides being chemically stable, being non-volatile, odorless materials, which do not cause environmental impacts [5]. The silsesquioxanes have a large number of applications, and this number increases when these structures are used as precursors in the formation of organic-inorganic hybrid materials [2, 6]. The applications of these materials include electronic devices [5], biosensors [3, 5, 6], catalysts [2, 5, 7, 8, 9], polymers [3, 5], fuel cells [2], liquid crystals [2, 3], optical fiber coatings [2], additives [2], optical devices [6], and silica interface precursors [10]. Electrodes chemically modified with silsesquioxane is uncomum are arousing great interest in the area of electrochemistry due to easy preparation and quick renewal of the electrode surface and by possibility of those materials act as electrochemical sensor and power electrocatalysts [11-14]. Many ways of anchoring compounds electrochemically active in the surface have been investigated in order to shorten the distance between the sites of oxidation-reduction involved in electronic transfer reactions [15,16].

In this paper we present the preparation, preliminary characterization and voltammetric studies of copper hexacyanoferrate (III) (CuHCF) obtained by the interaction with the functionalized Polyhedral Oligosilsesquioxane and 4-amino-5-4 (pyridyl)-4*H*-1,2,4-triazole-3-thiol (APTT) as peripheral organic group, described here as SA. The preparation of hybrid silsesquioxane was carried out by two stages. At the first stage, the SA adsorbs Cu^{2+} and the second step the composite formed (CuSA) reacts with hexacyanoferrate forming a new composite (CuHSA). After rigorous voltammetric

studies, the composite was tested in the electrocatalytic determination of nitrite. Nitrite is used as a food preservative; however, its excessive presence can be detrimental to health because of their possible carcinogenic effect. Thus, monitoring the amount of nitrite in a given environment is extremely important and electrochemical methods are effective alternative for this type of determination because of their properties with rapid response and simple use [17,18].

2. EXPERIMENTAL

2.1. Reagents

All reagents and solvents were of analytical grade (Alpha Aesar, Merck or Aldrich) and were used as purchased and deionized water, with Milli-Q Gradient system from Millipore was used. The solutions of sodium nitrite were prepared immediately before use.

2.2. Techniques

2.2.1. Fourier transform infrared spectra

Fourier transform infrared spectra were recorded on a Nicolet 5DXB FTIR 300 spectrometer. Approximately 600 mg of KBr was grounded in a mortar with a pestle, and sufficient solid sample was grounded with KBr to make a 1wt % mixture to produce KBr pellets. After the sample was loaded, the sample chamber was purged with nitrogen for at least 10 min. prior the data collection. A minimum of 32 scans was collected for each sample at a resolution of 4 cm^{-1}.

2.2.2. Electrochemical measurements

For cyclic voltammetric measurements was employed a potentiostat from Microchemistry, MQP1 model. The electrochemical system used was composed of three electrodes: platinum electrode used as auxiliar, Ag /$AgCl_{(s)}$ as a reference and modified graphite paste as a working electrode. The working electrode consists of a glass tube with 15 cm long, with a inner diameter of 0.30 cm and external diameter of 0.5 cm with the internal cavity connected by a copper wire to establish the electrical contact.

The cyclic voltammetry technique was employed to study the electrochemical behavior of composite (CuHSA). The catalytic current was established by the difference between the current measured in the presence of nitrite and in its absence.

2.3. Synthesis of octa-(3-chloropropyl) silsesquioxane (SS)

For the synthesis of octa-(3-chloropropyl)silsesquioxane (SS) (Fig. 1a) a procedure described in the literature was followed [19].

800 ml of methanol, 27.0 ml of hydrochloric acid (HCl) and 43.0 mL of 3-chloropropyliltriethoxysilane were added into a round bottom flask of 1000 mL. The system was kept under constant stirring at room temperature for 5 weeks. The solid phase was separated by filtration in a sintered plate funnel, yielding a white solid, octa-(3-chloropropyl)silsesquioxane (SS), which was then oven dried at 120 ºC for 4 hours. Figure 1a illustrates a representative scheme of this synthesis.

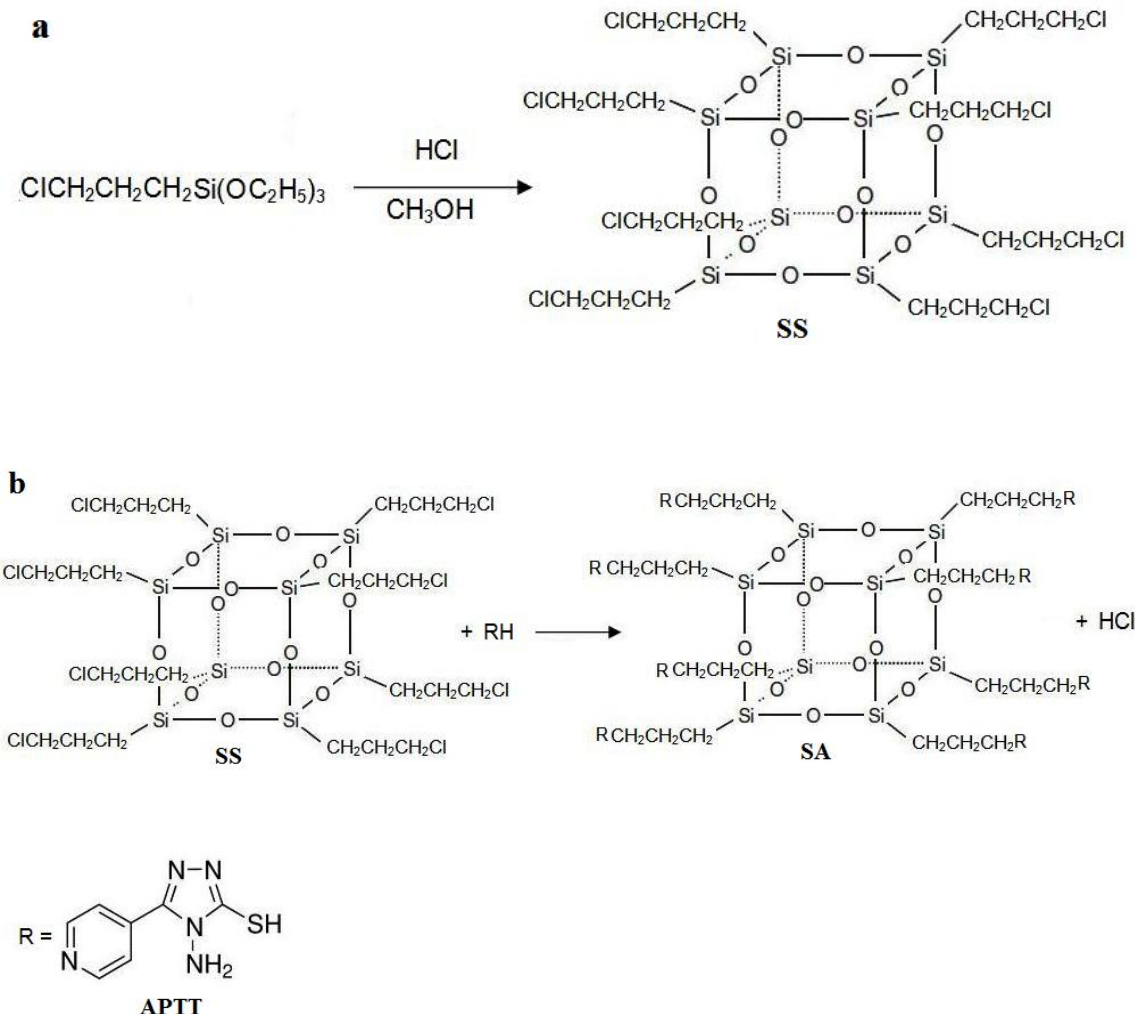

Figure 1. (a) Schematic representation of the preparation of octa-(3-chloropropyl)silsesquioxane [20-adapted] and (b) organofunctionalization of octa-(3-chloropropyl) silsesquioxane (SS) with the modifying agent APTT.

2.4. Functionalization of octa-(3-chloropropyl)silsesquioxane with APTT (SA)

The functionalization of octa-(3-chloropropyl)silsesquioxane (SS) (Fig. 1b (1)) was performed in a 3-neck flask of 500 mL containing 9.70×10^{-3} mol of SS, previously dried at 100 °C for 2 hours, 8.70×10^{-2} mol of APTT and approximately 200 mL of dimethylformamide (DMF). The mixture was refluxed at 150 °C with constant stirring for 96 hours. Then the solid phase was separated in a sintered funnel and washed in a Soxhlet extractor with DMF for 48 hours. The material obtained was oven

vacuum dried at 100 °C for 4 hours and described as SA (Fig. 1b (2)). Figure 1b schematically illustrates the organofunctionalization process of SS (a) with APTT (1b (3)).

2.5. Preparation of Copper Hexacyanoferrate with SA (CuHSA)

The complexes were prepared as follows: 1.00 g of SA was added to 25.0 mL of a solution of 1.0×10^{-3} mol L^{-1} $CuCl_2$ $5H_2O$. The mixture was stirred for 40 minutes at room temperature. The solid phase was then filtered and washed thoroughly with deionized water. The materials resulting from this first phase were oven dried at 70 ºC and designated as CuSA. In the second stage, the CuSA was added to a solution of 1.0×10^{-3} mol L^{-1} of potassium hexacyanoferrate (III) and the mixture was stirred for 40 minutes at room temperature and then the solid was thoroughly filtered, washed with deionized water and dry at room temperature. The materials resulting from this stage were described by CuHSA.

2.6. Preparation of Chemically modified carbon paste electrodes

The chemically modified carbon paste electrodes were prepared by mixing the modified silsesquioxane (CuHSA, 20.0 mg), graphite powder (80.0 mg), and nujol oil (25.0 μL). The electrode body was fabricated from a glass tube of i.d. 3 mm and height of 14 cm, containing graphite paste. A copper wire was inserted through the opposite end to establish electrical contact. After the mixture had been homogenized, the modified paste was carefully positioned on the tube tip to avoid possible air gaps, which often enhances electrode resistance. The external surface of the electrode was smoothed on soft paper. A new surface can be produced by scraping out the old surface and replacing the carbon paste.

3. RESULTS AND DISCUSSION

Figure 2 (a) refers to the spectrum of the APTT bond, showing characteristic bands of this ligand, which are the bands from 500 to 1600 cm^{-1}, referring to the vibrations of the APTT ring. Similar to the bands at ~1310, 1415 and 1550 cm^{-1} that correspond to the axial deformation C-N (υ C-N), the axial deformation C-N (υ C-N) of the cycle, and angular deformation of N-H (δ N-H) of the APTT ring, respectively. And in regions near to 1620 cm^{-1} there was a band attributed to the axial strain C=N (υ C=N). The band at ~2790 cm^{-1} corresponds to the vibration of the S–H bond (υ S-H), and the intense bandwidth is attributed to the O-H deformation of the molecules H_2O (υ O-H). Other absorption bands were observed, an intense broad band between 2300 and 2600 cm^{-1} which can be attributed to the axial deformation of C-H (υ C-H) of the ring and two other bands at ~3160 and ~3270cm^{-1} referring to the axial deformation N-H. (υ N-H) [21].

Figure 2 (b) illustrates the vibrational spectrum of the functionalized material (SA), showing bands that are characteristic of the precursor materials S and APTT, such as the bands at ~1120 cm^{-1} related to asymmetrical stretching Si-O-Si (υ Si-O-Si) that correspond to that found for a cage-shaped

structure of silsesquioxane, confirming that the cubic structure is maintained. The bands at ~ 2900 and 2950 cm^{-1} attributed to the C-H bond vibration (υ C-H) and the Si–H vibration (υ Si-C), respectively, and band width can be attributed to the O-H deformation of molecules H_2O (υ O-H). The bands between 1350 and 1650 cm^{-1} were attributed to the vibrations and deformations of the APTT ring [21]. An absence of the band at 590 cm^{-1} related to the C-Cl vibrations was also observed, therefore confirming the complete organofunctionalization of S with APTT.

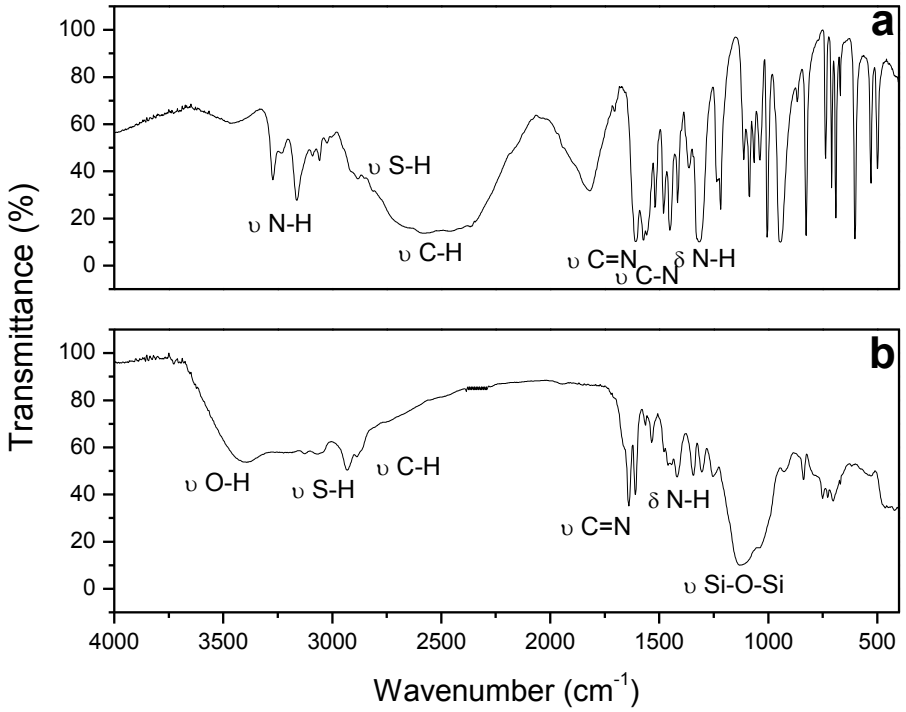

Figure 2. FT-IR of : (a) APTT and (b) SA.

Figure 3 shows the spectrum in the infrared region for the modified material CuHSA, CuSA and potassium hexacyanoferrate (III). The spectrum represented by Figure 3 (a) shows vibrations of hexacyanoferrate (III), where the most important vibrations are at ~ 2113 and 2026 cm^{-1}, which are vibrations related to the bonding vibrations of C≡N (υ C≡N). The spectra in Figure 3 (b and c) for CuHSA and CuSA, respectively, show typical vibrations of its precursor materials at ~1110 cm^{-1} for the asymmetric stretching Si-O-Si (υ Si-O-Si) which corresponds to the cage shaped structure of silsesquioxane. The bands at ~ 2900 and 2950 cm^{-1} are attributed to the vibration of C-H (υ C-H) bond and the S–H (υ S-H) vibration, respectively. The vibrations from 1200 to 1600 cm^{-1} are attributed to the vibrations of the APTT ring ligand (Figure 3 (c)). The spectrum represented by Figure 3 (b) of CuHSA showed the same corresponding vibrations, and also the vibration ~2100 cm^{-1}, which was attributed to C≡N (υ C≡N) stretching, characteristic of the transition metal hexacyanoferrate [21]. CuHSA was also characterized by cyclic voltammetry. The cyclic voltammogram of CuHSA presented a perfectly sharp redox pair with average potential $E^{\theta\prime}$ = 0.75 V where $E^{\theta\prime}$ (V) = (E_{pa} + E_{pc})/2

, attributed to the redox process $Fe^{(II)}(CN)_6$ / $Fe^{(III)}(CN)_6$ of the binuclear complex formed (CuHSA), and this value is very close to that described in the literature [22, 23]. Studies were conducted to determine the best composition of the electrode by varying the composition of the material modified with CuHSA and graphite, defined as the best concentration 20% (w/w) which showed an excellent voltammetric performance.

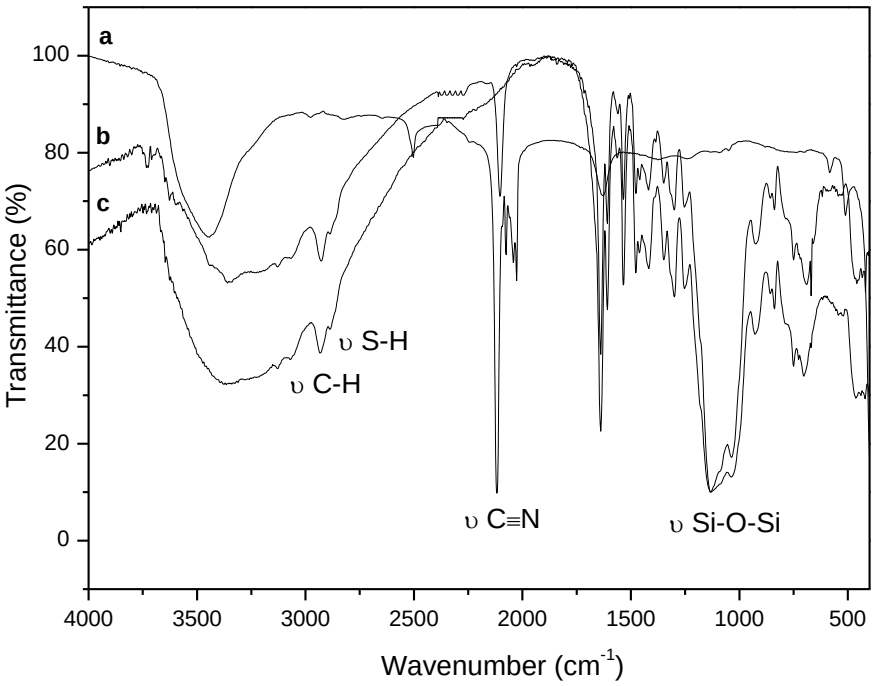

Figure 3. FT-IR of : a) Potassium hexacyanoferrate (III); b) CuHSA and c) CuSA.

Figure 4 illustrates the studies carried out on several supporting electrolytes of chloride (LiCl, NaCl, KCl and NH_4Cl) for studies on cations and (NO^-_3, Cl^- and SO_4^{2-}) for studies on anions. It was observed that the nature of the cations affected the average potential (E^{θ}') and the current intensities. It was also observed that the cyclic voltammograms of CuHSA in the presence of supporting electrolytes namely: NH_4Cl, KCl and NaCl (Figure 4 (b); (c) and (d)) showed well-defined redox pairs and that there was a shift in the average potentials (E^{θ}') to more positive potentials, in the following order: $NH_4^+ > K^+ > Na^+ > Li^+$, as shown in Table 1, which also lists the main electrochemical parameters of the compounds and their respective hydration radii. This new CuHSA material, as it is a compound analogous to Prussian blue, exhibits a zeolite structure type, showing cavities that allow the inflow and outflow of some alkaline metal ions with smaller hydration radii [24-26]. Thus, as the cations K^+ and NH_4^+ have smaller hydration radii (Table 1), they diffuse more easily between these cavities, resulting in a better electrochemical response of the modified electrode. With the data presented in Table 1, it was concluded that the electrode showed a better voltammetric profile in KCl than in NH_4Cl, as is also seen in Figure 4((a) and (d)), which can be explained by the low mobility of the NH_4^+ cation in relation to the K^+ cation [27]. Like the other cations studied (Li^+ and Na^+) have larger hydration diameters than

the cavity presented by CuHSA, the redox process is difficult, which is observed in the voltammetric response [28].

Figure 4 also shows that although the voltammetric performance is different only by one redox pair, in all cases it is verified with $E^{\theta'}$ = 0.75V and as already described, this redox pair was attributed to the $Fe^{II}(CN)_6/Fe^{III}(CN)_6$ process, and this value is very close to the one described in the literature for similar Prussian Blue [22].

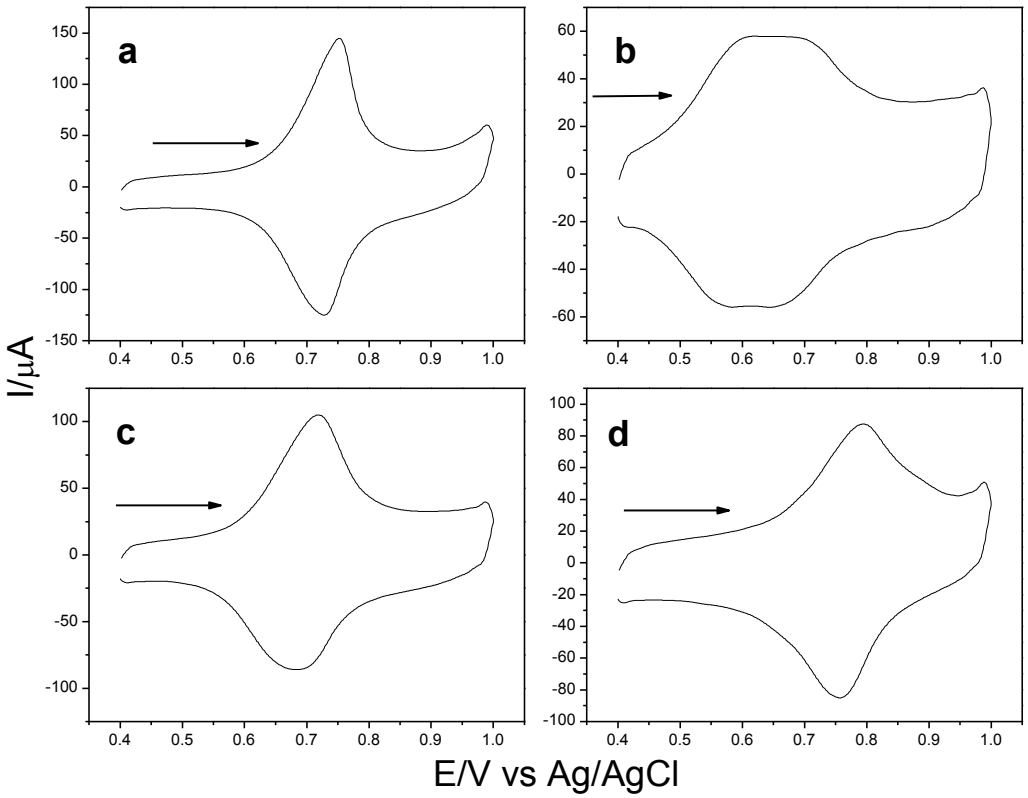

Figure 4. Cyclic voltammograms of graphite electrode modified with CuHSA: a) KCl, b) LiCl, c) NaCl, d) NH_4Cl (1.0 mol L^{-1}; v = 20 mV s^{-1}; 20% (w/w)).

Table 1. Relation of the diameter of hydrated cations with the electrochemical parameters of CuHSA*

Cation	[Ipa/Ipc]	$(E^{\theta'})_1$ (V)	ΔEp [Epa-Epc]	Diameter of Hydrated Cation (nm)**
Li^+	1.12	0.63	0.03	0.47
Na^+	1.20	0.70	0.03	0.36
K^+	1.11	0.74	0.02	0.24
NH_4^+	0.91	0.78	0.04	0.24

* 1.0 mol L^{-1}; v = 20 mVs^{-1}; 20%(w/w)).

** Ref. [29]

Analyzing Table 1 shows that the majority of the supporting electrolytes tested, the ratio Ipa/Ipc was very close to 1 and the potential change was of approximately 34 mV, which characterizes an quasi reversible system [30]. Due to the electrode exhibiting the best electrochemical parameters, in addition to its good voltammetric performance, KCl was chosen as the electrolyte to the other studies.

The cyclic voltammograms at different concentrations of KCl (considered the best electrolyte) were recorded in a concentration range from 1.0×10^{-3} to 2.0 mol L^{-1} and Figure 5 illustrates these studies.

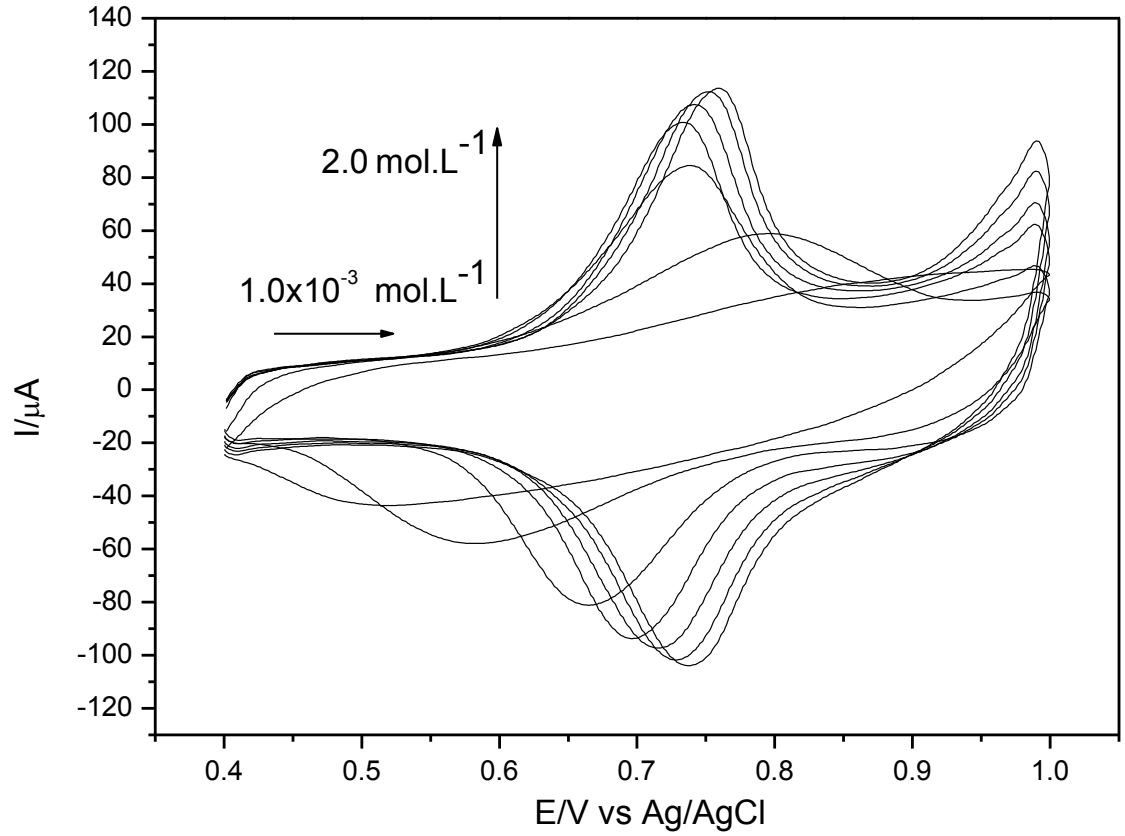

Figure 5. Cyclic voltammograms of the graphite paste electrode modified with CuHSA at different concentrations (KCl ; ν = 20 mV s^{-1}; 20% (w/w)).

Figure 6 illustrates that the average potential values ($E^{\theta'}$) shift linearly to more positive potentials by varying the KCl concentration from 1.0×10^{-3} to 2.0 mol L^{-1}, suggesting the involvement of the K^+ ion in the redox process. This study enabled to observe that for the graphite paste electrode modified with CuHSA, the line slope was of 56 mV per decade of potassium ions concentration, indicating a almost nerstian process [28]. To determine the aforementioned line slope only the voltammograms corresponding to concentrations 0.50 to 2.0 mol L^{-1} were used, because in this range, the redox processes are better defined, as shown in Table 2. With the results obtained in this study, the KCl concentration of 1.0 mol L^{-1} was determined as the best supporting electrolyte concentrations, due to the good voltammetric performance presented, in addition to having a good electrochemical stability

and reversibility reversibilidade (Ipa/Ipc ~ 1,0) and a small variation potential (ΔEp ~ 26 mV) where ΔEp (V) = $|E_{pa} - E_{pc}|$.

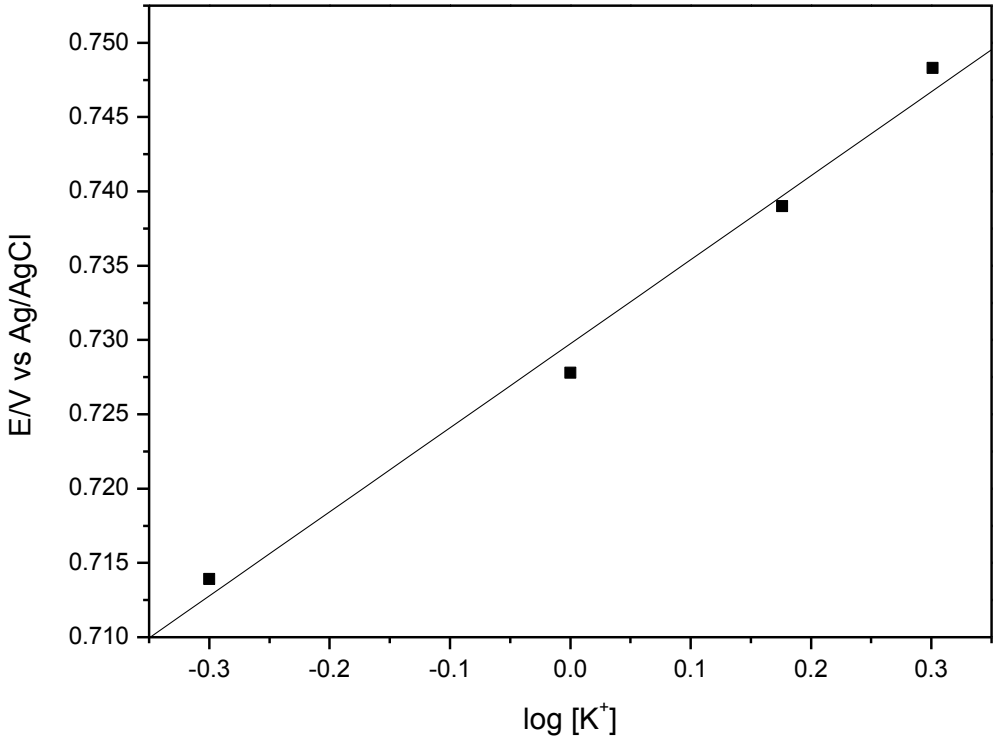

Figure 6. Average potential (E^{θ}') of graphite paste modified with CuHSA as a function of KCl concentration.

Table 2. Electrochemical parameters of CuHSA at different electrolyte concentrations (KCl; v = 20 mVs^{-1}; 20%(w/w)).

Concentration (mol L^{-1})	[Ipa/Ipc]	$(E^{\theta'})_1$ (V)	ΔEp (V) [Epa-Epc]
0.50	0.92	0.71	0.03
1.00	0.96	0.73	0.03
1.50	0.96	0.74	0.02
2.00	0.94	0.75	0.02

Figure 7 shows the cyclic voltammogram at different pH values (2-8). It is observed that by varying the hydrogen ion concentration there is no change in the anodic and cathodic peak current intensity but also in the other electrochemical parameters. Through this result pH 7 was chosen for the analytical system, since there is the intention of further studies for the electrocatalytic determination of drugs in biological pH (~7,1).

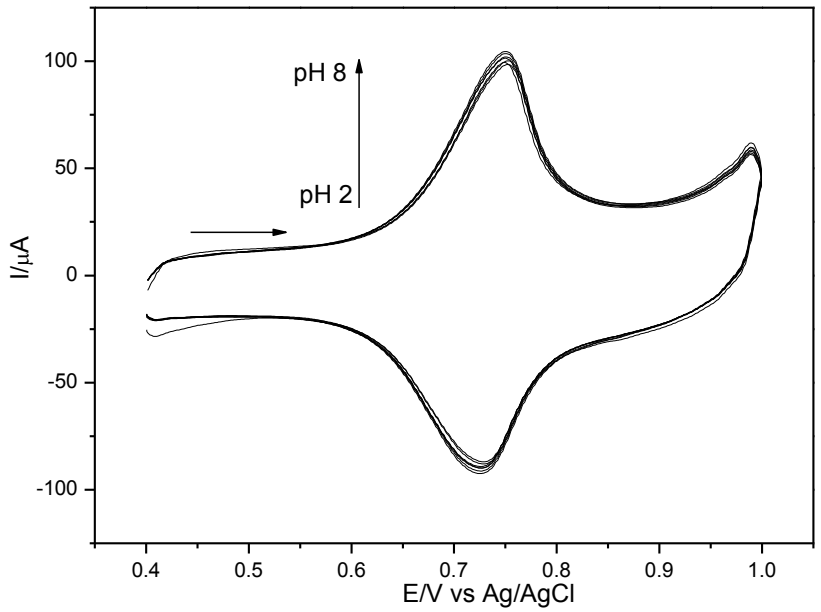

Figure 7. Cyclic voltammograms of graphite paste electrode modified with CuHSA at different pH values (20 mV s^{-1}; KCl 1.0 $molL^{-1}$; 20% (w/w)).

Figure 8 illustrates the cyclic voltammogram of CuHSA at different scan rates (10 to 100 mVs^{-1}). It was observed that by increasing the scan speed there is increased peak current and also a slight shift of the average potential to more positive values.

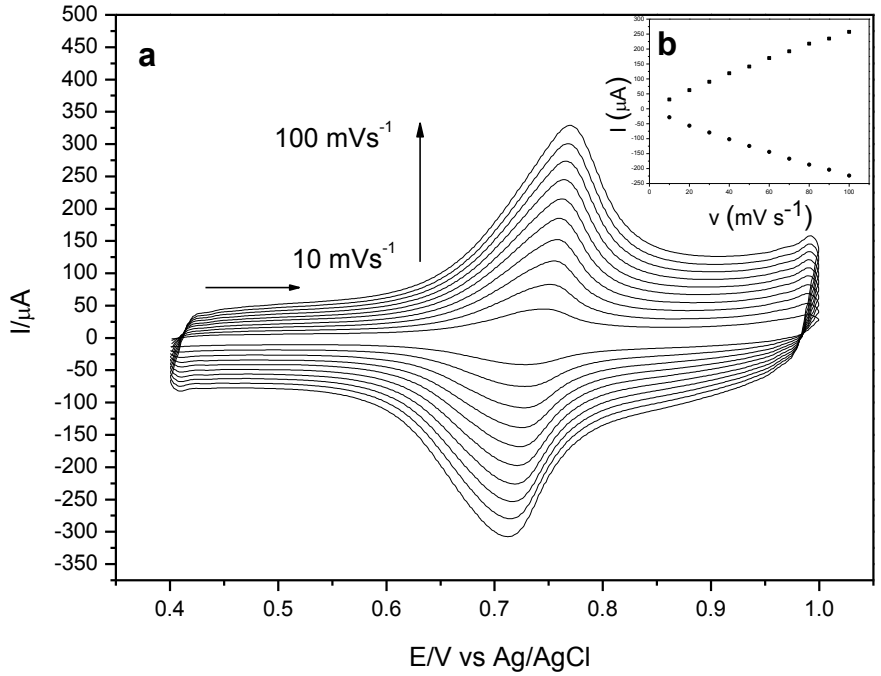

Figure 8. (a) Cyclic voltammograms of CuHSA at different scan rates (KCl 1.0 mol L^{-1}; 20% (w/w)) and (b) dependence of peak current intensity (anodic and cathodic) as a function of scan rate.

Table 3 shows the main electrochemical parameters of CuHSA at different scan rates. With the graph inserted into Figure 8 we observe a linear dependency between the current intensity of the anodic (R=0.998) and cathodic (R=0.998) peaks and the scan rate for the peak which characterizes an adsorptive process [30], as confirmed by previously presented adsorption studies [31].

Table 3. Electrochemical parameters of CuHSA at different scan rates (KCl 1.0 mol L^{-1}; pH 7.0; 20%(w/w)).

Scan rate ($mV\ s^{-1}$)	[Ipa/Ipc]	($E^{\theta'}$) (V)	ΔEp (V) [Epa-Epc]
10	1.01	0.73	0.02
20	1.10	0.74	0.02
30	1.14	0.74	0.03
40	1.17	0.74	0.03
50	1.14	0.74	0.03
60	1.18	0.74	0.04
70	1.15	0.74	0.04
80	1.17	0.74	0.05
90	1.15	0.74	0.05
100	1.15	0.74	0.06

3.1. Electrocatalytic oxidation of nitrite

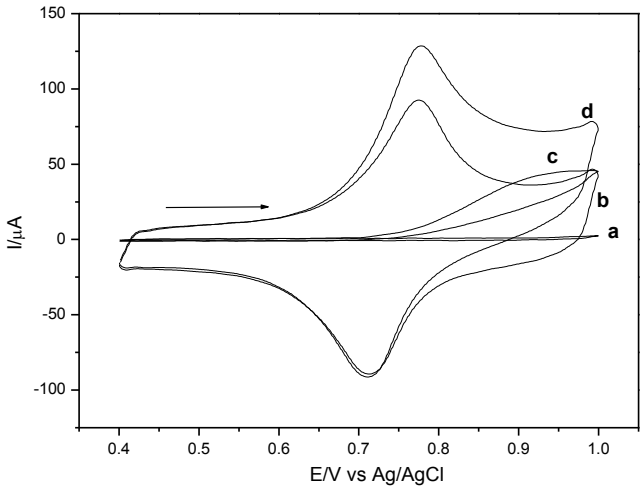

Figure 9. Cyclic voltammograms: a) of the graphite paste electrode, b) of the graphite paste electrode modified with CuHSA, c) of the graphite paste electrode in 1.0×10^{-3} mol L^{-1} of sodium nitrite, d) of the graphite paste electrode modified with CuHSA in 1.0×10^{-3} mol L^{-1} of sodium nitrite (KCl 1.0 mol L^{-1}; v = 20 mV s^{-1}; pH 7.0; 20%(w/w)).

Figure 9 illustrates the voltammetric behavior of the graphite paste electrode modified with CuHSA for the electro-oxidation of sodium nitrite in 1.0 mol L^{-1} KCl. The graphite paste electrode in a

solution of KCl 1.0 mol L^{-1} in the absence and presence of sodium nitrite did not show a redox pair in the potential range studied between 0.4 and 1.0 V (curve a and b, respectively). After the addition of sodium nitrite there was an increase in the anodic peak current intensity (curve d) when compared with the graphite paste electrode modified with CuHSA (curve c). There was an increase in the anodic current intensity of the peak at 0.77 V and a small shift to more negative potentials.

Figure 10 also illustrates that this current increase is proportional to the increasing concentration of sodium nitrite and this intensity increase of anodic current clearly shows the electrocatalytic oxidation of sodium nitrite by CuHSA.

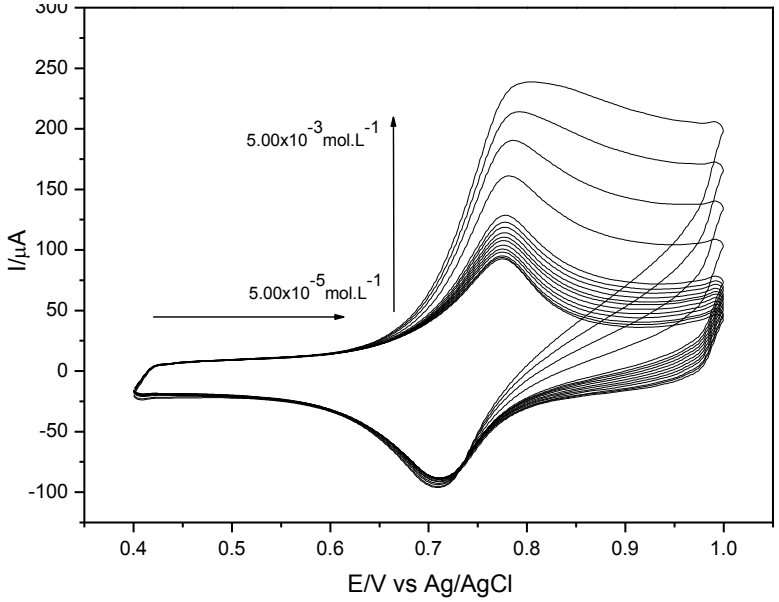

Figure 10. Cyclic voltammograms of the applications of varying concentrations of sodium nitrite using graphite paste electrode modified with CuHSA (KCl 1.0 mol L^{-1}; v = 20 mV s^{-1}; pH 7.0; 20% (w/w)).

The oxidation of nitrite proposed by Guidelli et al. [32] and Casella et al. [33] can be describes according to the following equation:

$$NO^-_2 + H_2O \longrightarrow NO_3^- + 2H^+ + 2e^- \quad (1)$$

And for this system the electrocatalytic process proposed for the electrode interface – solution is shown below:

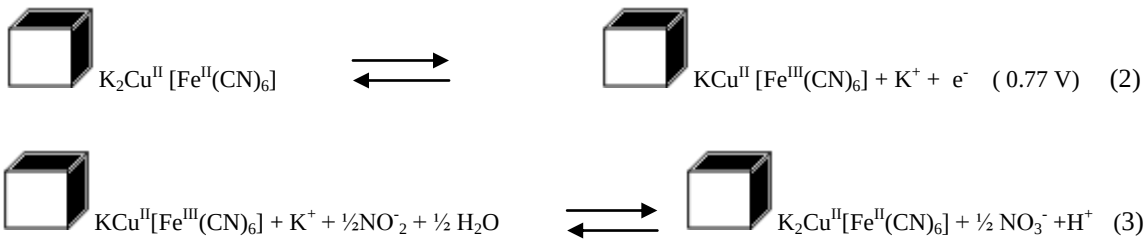

For this attribution an electro inactivity nature of silicate cage was considered [34]. The electrocatalytic oxidation of NO^-_2 occurs as showed by equations 1: Fe^{3+} produced during anodic scan, chemically oxidize the molecule NO^-_2 when it is reduced to Fe^{2+}, which will again be electrochemically oxidized to Fe^{3+}. The Electrochemical and chemical processes can be represented according to equations 2 and 3 respectively:

Figure 11 illustrates the analytic curve of the sodium nitrite concentration as a function of anode current for the peak. The modified electrode showed a linear response of 1.0×10^{-5} to 5.0×10^{-3} mol L^{-1} and an equation corresponding to Y(μA) = 76.51 + 30.005 [sodium nitrite] with a correlation coefficient of r = 0.99. The method has a detection limit of 3.57×10^{-4} mol L^{-1}, standard deviation of 1.5% for *n*=3 with an amperometric sensitivity 30.00 mA/mol L^{-1} to sodium nitrite. The modified electrodes were stable during all studies. The reproducibility was satisfactory for the investigated concentration range (RSD 2.3%) for nitrite. The influence of others biological substances, on the electrode response was examined. Interference studies were carried out by exposing the and 100 fold Ascorbic Acid, Glucose, Dopamine, Oxalic Acid, Citric Acid, Maltose, Levulose, Sucrose, and Tartaric acid but is stronger influencied by N-acetycysteine, L-cysteine dypirone (< 1 fold).

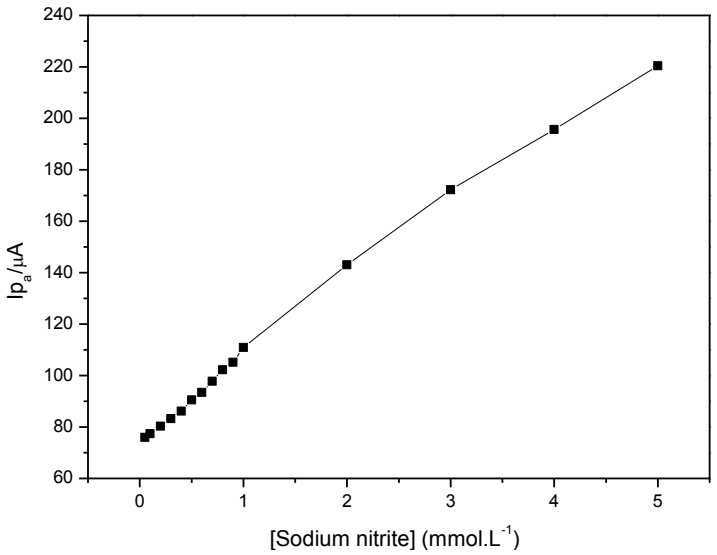

Figure 11. Analytical curve of the anodic peak for the determination of sodium nitrite using graphite paste electrode modified with CuHSA (KCl 1.0 mol L^{-1}; *v* = 20 mVs^{-1}; pH 7.0; 20%(w/w)).

4. CONCLUSION

Using a simple analysis of FT-IR and cyclic voltammetry we can conclude that SA, followed by an reaction of a metal ion (Cu^{2+}), interacte strongly with potassium hexacyanoferrate (III) forming a composite extremely electroactive (CuHSA). The cyclic voltammogram of the modified electrode containing CuHSA showed only one redox pair with $E^{\theta'}$= 0.75 V attributed to the redox process of the $Fe^{II}(CN)_6/Fe^{III}(CN)_6$ in the presence of binuclear complex formed. The modified

graphite paste electrodes were stable during all studies and presented an electrocatalytic activity for nitrite determination. The modified electrode showed a linear response of 1.0×10^{-5} to 5.0×10^{-3} mol L^{-1} and an equation corresponding to Y(μA) = 76.51 + 30.005 [sodium nitrite] with a correlation coefficient of r = 0.997. The method has a detection limit of 3.57×10^{-4} mol L^{-1}, standard deviation of 1.5% for n = 3 with an amperometric sensitivity 30.00 mA/mol L^{-1} to sodium nitrite. When compared to other electroanalytical methods, the main advantage of the modified electrode CuHSA is the facility of manufacture and the fact that it surface can be easily renewed. This feature is important when one wants to effectively implement various measurements in a short period of time. Another advantage is that it needs no prior chemical treatment. Additionaly the system could be employing in the direct determination of nitrite in presence of different ions and others biological substances.

ACKNOWLEDGEMENT
Financial support for this research was supplied by Fundação de Amparo à Pesquisa do Estado de São Paulo (FAPESP - Proc. 2012/05438-1 and 2012/11306-0) and Coordenação de Aperfeiçoamento de Pessoal de Nível Superior (CAPES).

References

1. G. Kickelbick, *Progress in Polymer Science*, 28 (2003) 83.
2. D. Gnanasekaran, K. Madhavan, B. S. R. Reddy, *Journal of Scientific and Industrial Research*, 68 (2009) 437.
3. D. B. Cordes, P. D. Lickiss, F. Rataboul, *Chemical Reviews*, 110 (2010) 2081.
4. R. H. Baney, M. Itoh, A. Sakakibara, T. Suzukit, *Chemical Reviews*, 95 (1995) 1409.
5. S. W. Kuo, F. C. Chang, *Progress in Polymer Science*, 36 (2011) 1649.
6. D. Xu, L. S. Loo, K. Wang, *Journal of Applied Polymer Science*, 122 (2011) 427.
7. G. Li, L. Wang, H. Ni, C. U. Pittman Junior, *Journal of Inorganic and Organometallic Polymers*, 11 (2001) 123.
8. A. Provatas, M. Luft, J. C. Mu, A. H. White, J. G. Matisons, B. W. Skelton, *Journal of Organometallic Chemistry*, 565 (1998) 159.
9. R. M. Laine, M. F. Roll, *Macromolecules*, 44 (2011) 1073.
10. M. Handke, A. Kowalewska, *Spectrochimica Acta, Part A: Molecular and Biomolecular Spectroscopy*, 79 (2011) 749.
11. D. R. Do Carmo, L. L. Paim, N. R. Stradiotto, *Materials Research Bulletin*, 47 (2012) 1028.
12. D. R. Do Carmo, L. L. Paim, D. R. Silvestrini, U. O. Bicalho, A. C. Sa, N. R. Stradiotto, *International Journal of Electrochemcal Science*, 6 (2011) 1175.
13. D. R. Do Carmo, L. L. Paim, G. Metzker, N. L. Dias Filho, N. R. Stradiotto, *Materials Research Bulletin*, 45 (2010) 1263.
14. T. F. S. Da Silveira, D. R. Silvestrini, U. O. Bicalho, D. R. Do Carmo, *International Journal Electrochemical Science*, 8 (2013) 872.
15. I. Willner, E. Katz, *Angewandte Chemie-international Edition*, 39 (2000) 1180.
16. R. W. Murray, Chemically Modified Electrodes. Bard A J, (ed). Electroanalytical Chemistry, Marcel Dekker, New York, 1984.
17. A. S. Adekunle, B. B. Mamba, B. O. Agboola, K. I. Ozoemena, *International Journal of Electrochemical Science*, 6 (2011) 4388.
18. C. Deng, J. Chen, Z. Nie, M. Yang, S. Si, *Thin Solid Films*, 520 (2012) 7026.
19. J. Chojnowski, W. Fortuniak, P. Ros´ciszewski, W. Werel, J. Łukasiak, W. Kamysz, R. Hałasa,

Journal of Inorganic and Organometallic Polymers and Materials, 16 (2006) 219.
20. D. R. Do Carmo, G. R. Castro, M. A. U. Martines, N. L. Dias Filho, N. R. Stradiotto, *Materials Research Bulletin*, 43 (2008) 3286.
21. R. M. Silverstein, F. X. Welbster, Spectrometric identification of organic compounds. John Wiley & Sons, New York, 1996.
22. M. R. Majidi, K. Asadpour-Zeynali, K. Shahmoradi, Y. Shivaeefar, *Journal of the Chinese Chemical Society*, 57 (2010) 391.
23. I. L. Mattos, L. Gorton, *Química Nova*, 24 (2001) 200.
24. D. Engel, E. W. Grabner, *Berichte der Bunsengesellschaft für physikalische Chemie*, 89 (1985) 982.
25. M. A. Maliki, P. J. Kulesza, *Electroanalysis*, 6 (1996) 113.
26. S. S. Narayanan, F. Scholz, *Electroanalysis*, 11 (1999) 465.
27. M. B. Soto, F. Scholz, *Journal of Electroanalytical Chemistry*, 528 (2002) 27.
28. A. P. Baioni, M. Vidotti, P. A. Fiorito, S. I. C. Torresi, *Journal of Electroanalytical Chemistry*, 622 (2008) 219.
29. D. Jayasri, S. Narayanan, *Sensors & Actuators, B: Chemical*, 119 (2006) 135.
30. A. L. Bard, L. R. Faulkner, Electrochemical methods: fundamentals and Applications. John Wiley & Sons, New York, 1980.
31. L. A. Soares, T. F. S. Da Silveira, D. R. Silvestrini, U. O. Bicalho, D. R. Do Carmo, *International Journal of Chemistry*, 5 (2013) 39.
32. R. Guidelli, F. Perdegola, G. Rospi, *Analytical Chemistry*, 44 (1972) 745.
33. I. G. Casella, A. M. Salvi, *Electroanalysis*, 9 (1997) 596.
34. D. R. Do Carmo, L. S. Guinesi, N. L. Dias Filho, N. R. Stradiotto, *Applied Surface Science*, 235 (2004) 449.